NOTES AND CORRESPONDENCE

On the Effect of Steep Slope Orientation on the Intensity of Daytime Upslope Flow

M. SEGAL

Department of Atmospheric Sciences, Colorado State University, Fort Collins, CO 80523

Y. OOKOUCHI

Yatsushiro National College of Technology, Yatsushiro 866, Japan

R. A. PIELKE

Department of Atmospheric Sciences, Colorado State University, Fort Collins, CO 80523

24 September 1986 and 30 April 1987

ABSTRACT

Steep north and south facing slopes may differ significantly in the amount of solar radiation received on their surfaces and consequently also in the related daytime induced thermal flows. This note provides a comparative analysis of the midday surface flows which developed on both slopes as a function of the slope steepness and the geographical latitude. The most significant differences between the two slopes were found on steep slopes in high latitudes during the winter. During the summer, the differences due to slope steepness and geographical latitude are relatively small. Numerical model simulations support the analysis results.

1. Introduction

In mesoscale evaluations (i.e., when the typical domain horizontal scale is around 100 km), the slope steepness and azimuth, as a rule, are not of major importance in the consideration of the amount of incoming solar radiation on a sloping surface (e.g., Mahrer and Pielke, 1977). However, this conclusion may not be correct if relatively smaller domains and steep slopes are considered. In these steep slope cases, for example, the amount of incoming solar radiation on a southern slope may differ significantly from that falling on an equivalent northerly facing slope. Since the incoming solar radiation provides the forcing which generates upslope daytime thermally induced flows, a pronounced difference is expected in those cases between flow intensities along the different slopes.

Early studies of mountain–valley daytime circulation involved with steep slopes are reviewed in Defant (1951). In recent years several studies, e.g., Whiteman (1982), Whiteman and McKee (1982), Banta and Cotton (1981), Bader and McKee (1983), Tang and Peng (1983), Banta (1984), and Post and Neff (1986) among others, have provided modeling and observational insight into the daylight hour development of upslope flows involved with steep slopes. In several of the aforementioned studies, attention was given to the effect of slope steepness and azimuth on the development of upslope flows, mostly during the transition from the nocturnal to daytime thermally induced flows. However, apparently no systematic attempt has been made to evaluate the daytime intensity of upslope flows as related to steep slope characteristics. Our note is an attempt in this direction by means of scale analysis. Emphasis is given to the evaluation of the effect of differences in the incoming solar radiation at the surface on the intensity of the midday developed surface flow, assuming a negligible synoptic flow. South and north facing slopes were considered for this purpose because they typically provide the maximum contrast of incoming solar radiation on the slope surfaces. The induced thermal flows along the slopes in both cases were compared and numerical model simulations were carried out to examine the analysis results.

2. Analysis

Three components which are relevant to our evaluation of the upslope thermally induced flow along steep terrain are scaled in this section. They consist of 1) the planetary boundary layer (PBL) depth, 2) the thermal induced flow intensity along the slopes, and 3) the incoming solar radiation on the southern and northern slopes.

a. Evaluation of the PBL depth

Let us consider a clear day situation. During the daytime hours a PBL of depth h_i is presumed to exist, where the major forcing for deepening of a convective PBL is the sensible turbulent heat flux at the surface. Adopting a simplified formulation, the height of the

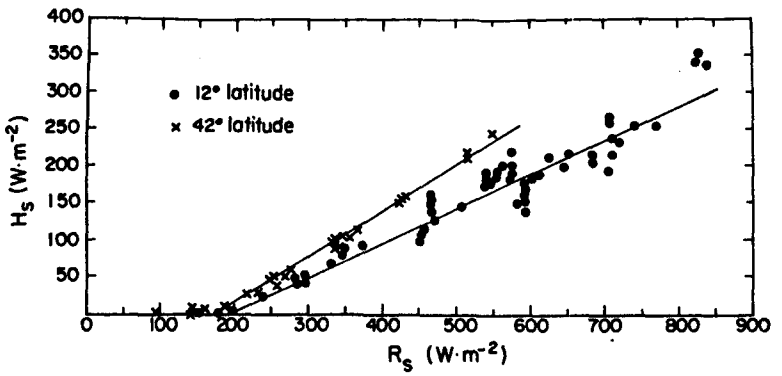

FIG. 1. Relation between the sensible heat (H_s) and the solar radiation incident on the surface (R_s), based on the model simulation described in section 3. Dots and X-marks relate to model simulations at 12° and 42°N latitudes, respectively.

PBL, h_i, at any time, t, following sunrise, can be approximated through the relationship

$$\frac{1}{\rho_a C_p}\int_0^t H_s dt \approx \frac{1}{2}\frac{\partial\theta_0}{\partial z}h_i^2 \tag{1}$$

where

H_s sensible heat flux
$\frac{\partial\theta_0}{\partial z}$ the initial potential temperature lapse
ρ_a air density
C_p specific heat of air at constant pressure.

It is assumed that the sensible heat flux, H_s, is related linearly through a factor k to the incoming global solar radiation at the surface, R_s, reduced by a minimal radiation, r, needed to produce a positive sensible heat flux from the surface to the atmosphere. The threshold shortwave flux r would be expected to vary with such parameters as soil wetness, soil thermal conductivity, etc. Figure 1 provides illustrations of the relation between H_s and R_s, based on model simulations at latitudes 12° and 42° as described in section 3. A closely linear relation is evident with the intercept $r \approx 180$ W m^{-2}; however, this slope differs somewhat between geographical locations, due to changes in atmospheric thermodynamic and soil thermal conditions at the different latitudes. Using (1) we obtain

$$h_i = \left[\frac{2\int_0^t H_s dt}{\rho_a C_p \frac{\partial\theta_0}{\partial z}}\right]^{1/2} \approx \left[\frac{2k\int_0^t R dt}{\rho_a C_p \frac{\partial\theta_0}{\partial z}}\right]^{1/2} \tag{2}$$

where $R = R_s - r$.

b. *The flow intensity along slopes*

The circulation theorem was utilized to evaluate the daylight thermally induced upslope. A circulation path whose upper section coincides with the PBL top was chosen (see Fig. 2 for an illustration). It is expected that the top path approximately separates the upslope and downslope portions of the circulation [see, for example, the observational study by Johnson and O'Brien (1973), or the model evaluations by Anthes (1978) and Mizzi and Pielke (1984)].

Following McNider and Pielke (1981), Segal et al. (1983), and Ookouchi et al. (1984), applying the circulation theorem along the path shown in Fig. 2 gives for the circulation time change:

$$\frac{\partial C}{\partial t} = \frac{\partial}{\partial t}\oint u dl$$
$$\approx \int_S \frac{\partial\theta_0}{\partial z}\cdot\frac{\partial z_G}{\partial x}\cdot\frac{g}{\theta}dS - \int_S \frac{\partial\theta'}{\partial x}\frac{g}{\theta}dS + \int_A^B F dl$$
$$\approx \frac{\partial\theta_0}{\partial z}\cdot\frac{\partial z_G}{\partial x}\cdot\frac{g}{\theta}\cdot L\cdot h_i - (\tilde{\theta}'_2 - \tilde{\theta}'_1)\frac{g}{\theta}\cdot h_i + \int_A^B F dl \tag{3}$$

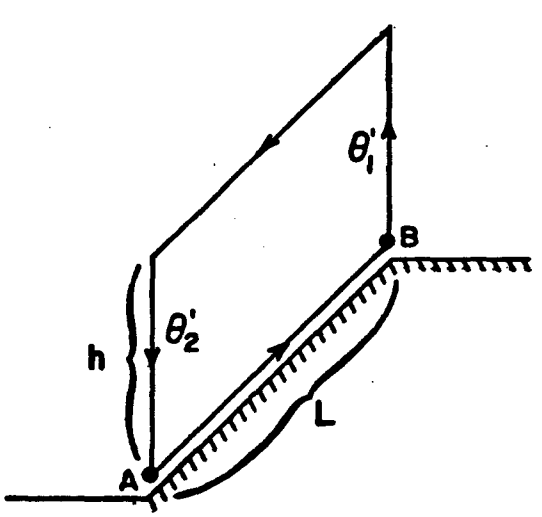

FIG. 2. Schematic illustration of the chosen path of integration for the circulation evaluation, L is the horizontal extent of the circulation path and h (the boundary layer depth) represents its vertical extension.

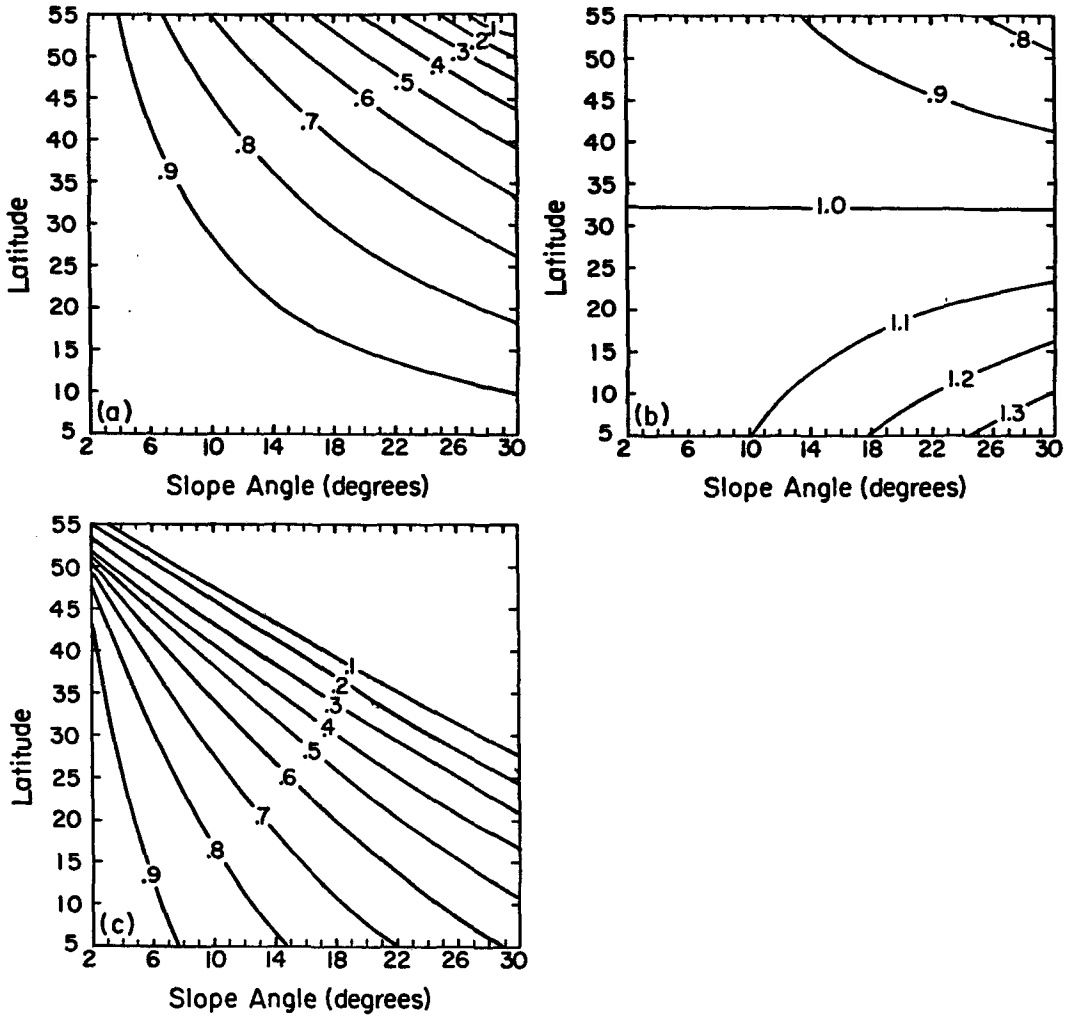

FIG. 3. Computed values of the north-to-south-facing slope circulation ratio R_c, based on Eq. (10), for various slope steepness and latitude for (a) 21 March sun, (b) 21 June sun, and (c) 21 December sun.

where

- u wind component along the circulation path
- $\frac{\partial z_G}{\partial x}$ the slope steepness
- g the gravity acceleration
- F friction on the lower section of the circulation path
- L the slope extent
- S the area enclosed within the path.

The tilde symbol indicates a vertically averaged value within the PBL while a prime indicates a deviation from the initial state.

Under the assumptions that (a) h_i is appreciably smaller than L (for example, when the lower atmosphere backward thermal stratification is relatively stable, or when the sensible heat fluxes are low) and (b) the mean vertical velocities involved with the circulation, C, are much smaller than the horizontal velocities, then the contribution of the vertical sections of the path to the circulation can be neglected. In addition, the upper section of the path experiences negligible wind speed because h_i is assumed to be the approximate boundary between the upslope flow layer and the return flow aloft. Therefore, we can use the following approximation:

$$\frac{\partial C}{\partial t} \approx \frac{\partial C_s}{\partial t} = \frac{\partial}{\partial t}\int_A^B u_s \cdot dl \tag{4}$$

where u_s is the upslope component of the flow along the lower path.

The friction term in (3) is presented in its Rayleigh form for the scaling purposes of this study:

$$F(u_s) = -\alpha u_s. \tag{5}$$

Additionally, the second term in Eq. (3) is negligible

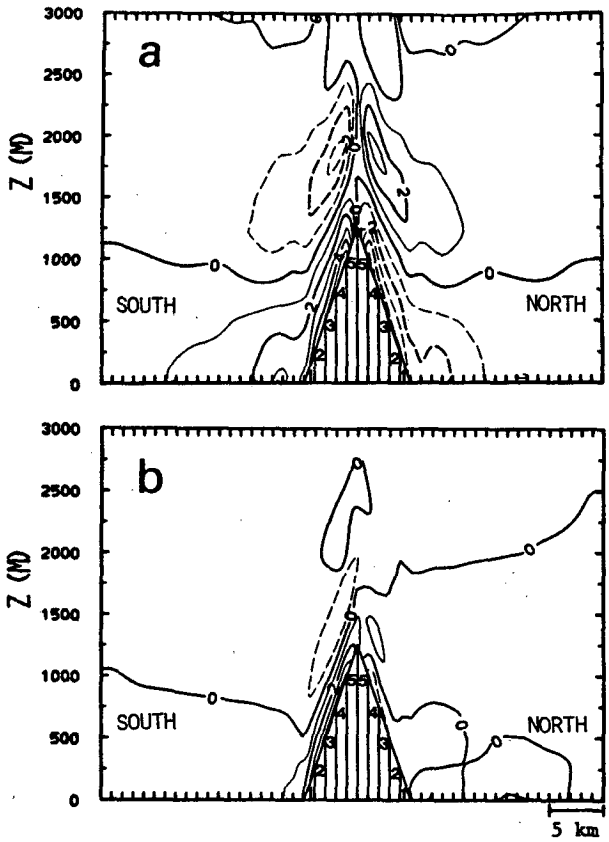

FIG. 4. Vertical cross section of the simulated domain presenting the south-north component of the wind, u, (m s^{-1}) at noon (1200 LST) for 21 December solar radiation for a 14° steep slope: (a) at latitude 12°N, (b) at latitude 42°N.

compared to the first one, because from scaling considerations the ratio of these two terms is

$$(\tilde{\theta}'_{02}-\tilde{\theta}'_{01})/(\theta_{02}-\theta_{01}) \approx O(10^{-1}) \tag{6}$$

where θ_{01} and θ_{02} are the upper slope and lower slope PBL potential temperature, respectively. Based on the foregoing two approximations and substituting the value of h_i from Eq. (2), integrating Eq. (3) with time provides the surface line circulation C_s following time t:

$$C_s=\int_A^B u_s dl|_t \approx L\frac{g}{\theta}\frac{\partial z_G}{\partial x}\left(2k\frac{\partial\theta_0}{\partial z}\right)^{1/2} \times(\rho_a C_p)^{-1/2}e^{-\alpha t}\int_0^t\left[e^{\alpha\tau}\cdot\left(\int_0^\tau R d\tau'\right)^{1/2}\right]d\tau. \tag{7}$$

For scaling purposes, we assume that $(\int_0^\tau R d\tau')^{1/2}$ varies linearly with time (i.e., between 0 in the morning and $R_0 = [\int_0^t R d\tau]^{1/2}$ at noon). Typically in our case, $\alpha \approx 10^{-3}$ and $t \approx 2\cdot 10^4$ s. Using these assumptions:

$$\int_0^t\left[e^{\alpha\tau}\cdot\left(\int_0^\tau R d\tau'\right)^{1/2}\right]d\tau=\frac{R_0}{\alpha}e^{\alpha t}-\frac{R_0}{t\alpha^2}e^{\alpha t}+\frac{R_0}{t\alpha^2} \approx \frac{R_0}{\alpha}\cdot e^{\alpha t}. \tag{8}$$

Therefore, the following approximation can then be derived for (7):

$$C_s=\int_A^B u_s dl|_t \approx \frac{L}{\alpha}\cdot\frac{g}{\theta}\cdot\frac{\partial z_G}{\partial x}\left(2k\frac{\partial\theta_0}{\partial z}\right)^{1/2}\cdot(\rho_a C_p)^{-1/2}\left[\int_0^t R d\tau\right]^{1/2}. \tag{9}$$

When assuming that R acquires a sinusoidal variation, integrating (7) numerically indicates that the approximation given by (8) (with the aforementioned values of α and t) results in an error of less than 5%. From Eq. (9) the ratio R_c of the line surface circulation along a north facing slope as compared to that on an adjacent equivalent south facing slope can be approximated at a given time t following sunrise as

$$R_c=\frac{C_s|_N}{C_s|_S} \approx \left[\frac{\int_0^t R d\tau|_N}{\int_0^t R d\tau|_S}\right]^{1/2}. \tag{10}$$

Since, as stated previously, the purpose of the current note is to compare the thermally induced flows on steep north and south-facing slopes, Eq. (10) implies that the square root of the time-integrated modified incoming solar radiation, R, on both slopes has to be compared. In section 3 the needed radiation characteristics are computed, from which a comparison of circulation intensity between north and south-facing slopes can be made.

Using the Atwater and Ball (1978) formulation for computation of solar radiation, R_s, on tilted surfaces, we computed the modified incoming solar radiation R. Typical atmospheric moisture profiles (as function of month and latitude) which were needed for these

TABLE 1. Main model input parameters for the simulated cases.

Roughness parameter	4 cm
Albedo	0.2
Background potential temperature lapse	4 K/1000 m
Day of the year	21 December
Soil moisture availability	0.07
Initial surface moisture	
Lat. 12°N	15 g kg^{-1}
Lat. 42°N	5 g kg^{-1}
Initial surface temperature	
Lat. 12°N	300 K
Lat. 42°N	283 K
Horizontal grid interval	1 km
Time step	7.5 s

TABLE 2. The south–north component of the surface wind (u_s) at several slope points (indicated in Fig. 4), the surface line circulation, and the circulation ratio R_C as obtained from the numerical model simulations.

Latitude (N)	Slope	u_s (cm s^{-1}) 1	2	3	4	5	$\int \lvert u_s \rvert dl$	R_C
12°	North	−246	−379	−401	−445	−493	1964	0.87
	South	299	439	467	536	506	2247	
42°	North	−9	−83	−88	−149	−149	478	0.27
	South	212	349	391	408	385	1745	

computations were adopted from Oort and Rusmusson (1971). In the computations of the ratio R_c, a value for $r = 180$ W m^{-2} was chosen as suggested by Fig. 1, which is representative for both high and low latitude slope cases. Integrations of R in time on south and north facing slopes were carried out for the sunrise to noon period in order to calculate the noon values of the ratio R_c based on Eq. (10). Figure 3 presents the noon hour values of R_c (when the upslope flows are approaching their peak values) as dependent on geographical latitudes and slope inclination angles, for the twenty-first day of December, March and June. They indicate a possible substantial difference in the intensity of north and south facing slope flows during the winter months, with the difference increasing with slope steepness and latitude. During the summer the intensity of the surface line circulation for both slopes is similar.

3. Numerical model simulations

In order to evaluate the scaling introduced in section 2, two-dimensional numerical model simulations were carried out for two cases. The numerical model used is that described in Mahrer and Pielke (1977) and McNider and Pielke (1981). Two illustrative simulations were carried out for 21 December at (i) latitude 12°N, and (ii) latitude 42°N. The simulations considered were, for simplicity, a single ridge with south and north facing slopes of a steepness of 14°, rather than performing simulations involved with each slope separately (see Fig. 4). The two cases provide examples for situations with relatively high and low values of R_c, respectively. Table 1 provides the main input parameters used in the model simulations. In the simulations the atmospheric moisture was changed with latitude in an equivalent manner to that adopted in the analytical derivation of the R_c values. The initial surface temperature at 12°N latitude is higher as compared to that at 42°N latitude. However, since the potential temperature vertical gradient at both latitudes is identical, the simulated flow intensity in both cases can be directly compared. The simulations began following sunrise, assuming no synoptic flow.

Figure 4 presents the simulated south–north wind component, denoted by u, for these cases. The values of the along-ridge velocity component (i.e., west–east), are relatively small and are not shown. For the 12°N latitude case, the u component wind developed along the northern slope is somewhat smaller than that along the southern slope. From Table 2, the simulation-computed ratio of surface line circulation along both slopes is 0.87, in reasonable agreement with the value of ~0.75 based on Fig. 3. For the 42°N latitude simulation, the developed upslope flows are weaker than in the 12°N latitude simulation, but with the south facing slope the flow is pronouncedly stronger and deeper than along the north facing slope. For this case $R_c = 0.27$ (Table 2), based on simulation results. While the scale analysis value derived from Fig. 3 (~0.2) is somewhat lower for this slope and latitude than in the simulation, a reduction of only about 2° in the slope steepness or in the latitude provides agreement between the scale analysis estimate of R_c and the simulated value for R_c from Fig. 4 and Table 2. Considering the approximations involved with the scaling procedures, it appears that the analysis in section 2 provides a procedure to reasonably estimate the ratio R_c in clear skies and negligible synoptic flow cases.

Finally, for the specific terrain configuration selected for the numerical simulations, in addition to the upslope thermal flow, an induced circulation (similar to a sea breeze) should occur to some degree between the relatively more warm south slope and relatively cold north slope (in the Northern Hemisphere). Such circulations are also anticipated between the adjacent flat plain and the slopes. However, as can be noted from Fig. 4, their alteration of the upslope thermal flow structure in these simulations is insignificant (see Ookouchi et al., 1984, for analyses of similar situations).

4. Conclusions

A comparative evaluation of daytime thermally induced surface flows along equivalent north- and south-facing steep slopes suggests 1) the most significant differences in their intensity occur during the winter, and in northern latitudes; and 2) a similar flow intensity for both slopes occurs during the summer for almost all steepnesses and latitudes. Both scale analysis and simulation results are provided for noon, when the upslope flows are matured and approaching their daytime

peak. Reasonable agreement is obtained between the scale analysis and the numerical model simulation results.

Finally, the analysis results suggest that the steepness of terrain within a mesoscale or larger-sized domain is an insignificant factor in modifying daytime thermal flows when solar radiation is considered. Typically, such domains are of horizontal scale of $\sim$100 km or more. Assuming, for example, a relatively significant elevation change of 2 km across the domain, the terrain inclination angle is only about 1°. According to the analysis presented in this note, for such low-terrain tilt angles the value of $R_c \approx 1$ is typical.

Acknowledgments. The study was supported by EPRI Grant RP-1630-53, by NPS grant NA81RAH0001, and by NSF Grant ATM-8414181 and ATM-8616662. The computations were carried out by the NCAR Computer Facility (NCAR is sponsored by the NSF). We would like to thank R. Arritt for useful discussions and the anonymous reviewers for their comments, and Sandy Wittler for the preparation of the manuscript.

REFERENCES

Anthes, R. A., 1978: The height of the planetary boundary layer and the production of circulation in a sea breeze model. *J. Atmos. Sci.*, **35**, 1231–1239.

Atwater, M. A., and J. T. Ball, 1978: A numerical solar radiation model based on standard meteorological observations. *Solar Energy*, **21**, 163–170.

Bader, D. C., and T. B. McKee, 1983: Dynamical model simulation of the morning boundary layer development in deep mountain valleys. *J. Climate. Appl. Meteor.*, **22**, 341–351.

Banta, R. M., and W. R. Cotton, 1981: An analysis of the structure of local wind systems in a broad mountain basin. *J. Appl. Meteor.*, **20**, 1255–1256.

——, 1984: Daytime boundary-layer evolution over mountainous terrain. Part I: Observations of the dry circulations. *Mon. Wea. Rev.*, **112**, 340–356.

Defant, F., 1951: Local winds, *Compendium of Meteorology*. T. F. Malone, Ed., 655–672, Amer. Meteor. Soc., Boston, MA.

Johnson, A., and J. J. O'Brien, 1973: A study of an Oregon sea breeze event. *J. Appl. Meteor.*, **12**, 1267–1283.

Mahrer, Y., and R. A. Pielke, 1977: The effects of topography on the sea and land breezes in a two-dimensional numerical model. *Mon. Wea. Rev.*, **105**, 1151–1162.

McNider, R. T., and R. A. Pielke, 1981: Diurnal boundary-layer development over sloping terrain. *J. Atmos. Sci.*, **38**, 2198–2212.

Mizzi, A. P., and R. A. Pielke, 1984: A numerical study of the mesoscale atmospheric circulation observed during a coastal upwelling event on 23 August 1972. Part I: Sensitivity studies. *Mon. Wea. Rev.*, **112**, 76–90.

Ookouchi, Y., M. Segal, K. C. Kessler and R. A. Pielke, 1984: Evaluation of soil moisture effects on the generation and modifications at mesoscale circulations. *Mon. Wea. Rev.*, **112**, 2281–2292.

Oort, A. H., and E. M. Rusmusson, 1971: Atmospheric circulation statistics. NOAA professional paper No. 5, NOAA, U.S. Department of Commerce, Washington, D.C., 323 pp.

Post, M. J., and W. D. Neff, 1986: Doppler lidar measurements of winds in a narrow mountain valley. *Bull. Amer. Meteor. Soc.*, **67**, 274–281.

Segal, M., Y. Mahrer and R. A. Pielke, 1983: A study of the meteorological patterns associated with a lake confined by mountains—The Dead Sea case. *Quart J. Roy. Meteor. Soc.*, **109**, 549–564.

Tang, W., and L. Peng, 1983: A numerical model of slopewind circulation regimes in a V-shaped valley. *Arch. Meteor. Geophys. Bioklim. Ser. B*, **32**, 361–380.

Whiteman, C. D., 1982: Breakup of temperature inversions in deep mountain valleys: Part I. Observations. *J. Appl. Meteor.*, **21**, 270–289.

——, and T. B. McKee, 1982: Breakup of temperature inversions in deep mountain valleys: Part II. Thermodynamic model. *J. Appl. Meteor.*, **21**, 290–302.